Chinese Chemical Letters 34 (2023) 107784

Contents lists available at ScienceDirect

Chinese Chemical Letters

journal homepage: www.elsevier.com/locate/cclet

Recent advances in zinc-ion hybrid energy storage: Coloring high-power capacitors with battery-level energy

Ling Miao[a], Yaokang Lv[b], Dazhang Zhu[a,*], Liangchun Li[a,*], Lihua Gan[a,*], Mingxian Liu[a,*]

[a] Department of Chemistry, Shanghai Key Laboratory of Chemical Assessment and Sustainability, School of Chemical Science and Engineering, Tongji University, Shanghai 200092, China

[b] College of Chemical Engineering, Zhejiang University of Technology, Hangzhou 310014, China

A R T I C L E I N F O

Article history:
Received 18 July 2022
Revised 14 August 2022
Accepted 24 August 2022
Available online 28 August 2022

Keywords:
Zinc-ion hybrid capacitor
Capacitor-type electrode
Battery-type electrode
Capacity/dynamics mismatch
Zinc-based electrolyte
Hybrid energy storage mechanism

A B S T R A C T

Zinc-ion hybrid capacitors (ZICs) are considered as newly-emerging and competitive candidates for energy storage devices due to the integration of characteristic capacitor-level power and complementary battery-level energy. The practical application of rising ZICs still faces the specific capacity and dynamics mismatch between the two electrodes with different energy storage mechanisms, which cannot meet the ever-growing indicator demand for portable electronic displays and public traffic facilities. Focusing on these unresolved issues, this mini-review presents recent advances in ZICs referring to the hybrid energy storage mechanism, design strategies of both capacitor-type and battery-type electrode materials, and electrolyte research toward advanced performances (*e.g.*, high operational potential, wide adaptive temperature). Finally, current challenges and future outlook have been proposed to guide further exploration of next-generation ZICs with a combination of high-power delivery, high-energy output and high-quality service durability.

1. Introduction

The fast-changing development of portable electronic displays and public traffic facilities has accelerated research advances in high-performance energy storage devices including supercapacitors, metal-ion batteries and their hybrid systems [1–3]. In supercapacitors, the energy storage is realized by means of interfacial cation/anion sorption in the Helmholtz double layers or surface pseudocapacitive reaction [1,4]; the capacitor-type working mechanism merely occurring on the electrode (near-)surface gives supercapacitors with remarkable power density, and the well-maintained electrode structure upon high-rate/successive charging-discharging turns also contributes to a long service lifespan [4,5]. On the contrary, the energy in metal-ion batteries is stored based on the intercalation/deintercalation reaction of cations into the internal electrode structure, which reveals a diffusion-dominated electrochemical process with remarkable energy density [3,6]; meanwhile, the structure distortion induced by the phase evolution of the battery material also degrades the cycling durability of metal-ion batteries [6–8].

Zinc-ion hybrid capacitors (ZICs) are considered as newly-emerging and competitive candidates for energy storage devices by coupling the characteristic capacitor-level power with complementary high energy of zinc-ion batteries [9–15]. Among various multivalent metal-based devices, more attention to zinc-based systems results from the overwhelming superiorities of Zn element: (1) natural abundance and massive production; (2) high theoretical gravimetric capacity of 820 mAh/g, as well as high compatibility and stability in aqueous solutions; (3) low electrochemical potential of −0.763 V (*vs.* the standard hydrogen electrode) and the two-electron redox property offering a high-energy density; (4) high safety and nontoxic nature [3,16]. Thus far, ZICs are defined as the hybrid system consisting of a capacitor-type electrode and a battery-type electrode in a zinc-based (*e.g.*, $ZnCl_2$, $Zn(CF_3SO_3)_2$, $ZnSO_4$, $Zn(NO_3)_2$, $ZnAc_2$, $Zn(ClO_4)_2$) electrolyte solution (Fig. 1) [6,10,13,16–20]. In ZICs, the capacitor-type electrodes (*e.g.*, double-layer capacitive carbons, pseudocapacitive materials) inherit the characteristic power/cycling merits of supercapacitors based on a surface-dominated charge-storage mechanism [12,17,19,21]. Compared with conventional ZICs merely using metal Zn as the anode, such broadly-defined ZICs using other battery-type electrode materials (*e.g.*, Mn/V-based oxides, Prussian blue analogues, organic compounds) promise complementary high-energy density relying on Zn^{2+} insertion/extraction into the crystal structure instead of Zn^{2+} deposition/stripping on the Zn anode [10,13,22,23]. However,

* Corresponding authors.
E-mail addresses: zhudz@tongji.edu.cn (D. Zhu), lilc@tongji.edu.cn (L. Li), ganlh@tongji.edu.cn (L. Gan), liumx@tongji.edu.cn (M. Liu).

https://doi.org/10.1016/j.cclet.2022.107784
1001-8417/

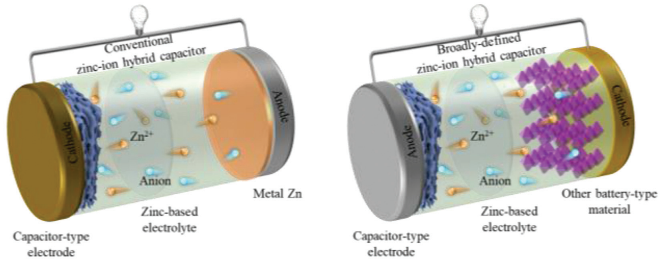

Fig. 1. Schematic representation of zinc-ion hybrid capacitors.

the practical application of rising ZICs still faces the specific capacity and dynamics (diffusion rate) mismatch between the two electrodes with different surface/diffusion-dominated energy storage mechanisms [6,19,24].

Focusing on these unresolved issues, great research efforts have recently been devoted toward upgrading the performances of present electrodes/electrolytes and exploring novel and high-quality active constituents in ZICs; in other words, the capacitor-type electrodes should increase the electrochemical active surface area by nanostructure engineering (surface accessibility) or doping redox-active constituents (surface pseudocapacitance) to bridge the capacity gap, and the battery-type electrodes should be tailor-designed by surface modification or architecture exploration to accelerate ion/electron diffusion rate in aqueous/non-aqueous electrolytes, thus aiming to matching high power and high energy simultaneously. This mini-review presents recent advances in ZICs referring to the hybrid energy storage mechanism, design strategies of both capacitor-type and battery-type electrode materials, and electrolyte research toward advanced performances (*e.g.*, high operational potential, wide adaptive temperature). Finally, current challenges and future outlook have been proposed for further exploration of next-generation ZICs.

2. Capacitor-type electrodes in high-power ZICs

Capacitor-type electrodes store energy by means of physical cation/anion sorption or redox pseudocapacitive reaction on the electrode (near-)surface, and are divided into double-layer capacitive carbons and pseudocapacitive materials. The surface-dominated working mechanism contributes to high-power delivery, wherein the specific capacity is unsatisfactory because of the relatively low surface utilization on electrochemical turns [2,6,25]. Therefore, great research efforts have been devoted toward increasing the electrochemical active surface area by nanostructure engineering (surface accessibility) or doping redox-active constituents (surface pseudocapacitance) to fabricate high-capacity capacitor-type electrodes without sacrificing the high-power density inherent to supercapacitors.

2.1. Double-layer capacitive carbons

Large-surface-area carbon-based materials featuring bonus conductivity/stability merits, have been commonly applied as the capacitor-type electrodes in ZICs, where large carbon surfaces can ensure considerable sorption capacity of cations/anions through the generation of the Helmholtz double layers [4,12,19,26,27]. Unfortunately, the electrolyte-accessible carbon surface upon actual electrochemical turns is far less than the specific surface area parameter measured under the gaseous atmosphere [2,25,28]. Consequently, an effective solution to gain high specific capacity is nanostructure engineering of carbon-based electrodes for improved electrochemical surface accessibility, including activated carbons (ACs), porous carbons, hollow carbon spheres, 2D graphene/carbon nanosheets, 1D carbon nanotubes (CNTs)/carbon nanofibers, *etc.* [10,12,19,27–34]. In terms of porous structure engineering, customized design of hierarchical porous carbon materials (HPCs) is highly praised as the alternative electrode to commercial AC products in current ZICs [29,35–39]. Interconnected meso-/macropores in HPCs can decrease the interfacial resistance as electrolyte-diffusion shortcuts into deep sorption sites (*i.e.*, micropores) on the interior surface, thus improving surface accessibility and specific capacity [35,36,40]. For instance, Wang's group prepared a metal-organic framework (MOF) as the precursor to obtain sharpened pencil-like HPC as a capacitive electrode in ZICs, and multi-level pore distribution offered sufficient storage and rapid transfer rate, thus achieving high-energy delivery of 130.1 Wh/kg for the as-built HPC//Zn device [29]. Xu's group reported the gas-steamed MOF synthesis to prepare porous carbon cages with large openings on their walls [34]. Active sites exposed on its unique open-wall structure guaranteed high-speed mass transfer of electrolyte-ions to the accessible surface, thus achieving a remarkable capacity of 225 mAh/g at 0.1 A/g for the coin-type ZIC cell. In terms of dimensional structure engineering, sp^2 carbon-based materials like graphene and CNTs also hold great promise as capacitive electrodes especially for portable ZICs, because of their prominent electrical conductivity, outstanding mechanical flexibility/resilience and accessible pores on the open surface [10,19,31,41–43]. In 2016, CNTs were paired as the cathode with a Zn anode into a $ZnSO_4$-based ZIC, in which a specific capacitance of 20 mF/cm^2 @ 10 mV/s and a stable cycling performance (up to 5000 cycles) were demonstrated [10]. Very recently, the surface chemistry of reduce graphene oxide cathode was regulated to upgrade the charge-storage capacity (245 F/g@0.5 A/g), and an energy density of 266 $\mu Wh/cm^2$ was realized for the 3D printed ZIC configuration [31]. Both experimental results and theoretical calculations confirmed reversible H^+ sorption and charge transfer on C atoms of the graphitic domains accompanied by the sp^2-sp^3 re-hybridization and the domain distortion/restoration (Fig. 2a), giving a supplementary capacity contribution beyond O-containing functionalities.

2.2. Pseudocapacitive materials

Pseudocapacitive materials with the co-contribution of both redox pseudocapacitive reaction and physical ion sorption become another strategy to increase the electrochemical active surface area for high specific capacity [17,24,44,45]. Redox pseudocapacitance can be doped by the reversible Faraday reaction between electrolyte-ions and redox-active constituents within a (*quasi*-)2D space of the electrode surface [6,7,46,47]. Pseudocapacitive electrode materials used in current ZICs mainly include redox-active carbonaceous frameworks, silicene, phosphorene and transition metal compounds like RuO_2, NbPO, $BiCuS_{2.5}$, MXenes [17,24,28,34,38,44,48–60]. For instance, Lu's group designed a N/O co-doped HPC as the cathode for a high-performance ZIC with a capacity of 177.8 mAh/g@4.2 A/g and an energy density up to 107.3 Wh/kg [38]. N dopants were evidenced to promote the surface chemical Zn^{2+} sorption *via* redox pseudocapacitive reaction of O-containing functionalities, finally replenishing the extra pseudocapacitance of the as-assembled N/O co-doped HPC//Zn device through C-O-Zn bonding (cathode: $C\text{-}OH + Zn^{2+} + e^- \leftrightarrow C\text{-}O\text{-}Zn + H^+$). Alshareef's group attributed the pseudocapacitance of the O-doped porous carbon cathode to the Zn^{2+}/H^+ co-action storage mechanism (Fig. 2b), where hydrogen redox reaction occurred during the discharge process (0.25-0 V) and oxygen pseudocapacitive reaction took action under a high potential of about 1.7-1.9 V [17]. And the H^+ consumption left behind a dynamic local OH^- environment reacting with Zn^{2+} for the precipitation/dissolution of byproducts (alkaline zinc salts). Beyond redox-active carbonaceous frameworks, transition metal compounds are also widely-

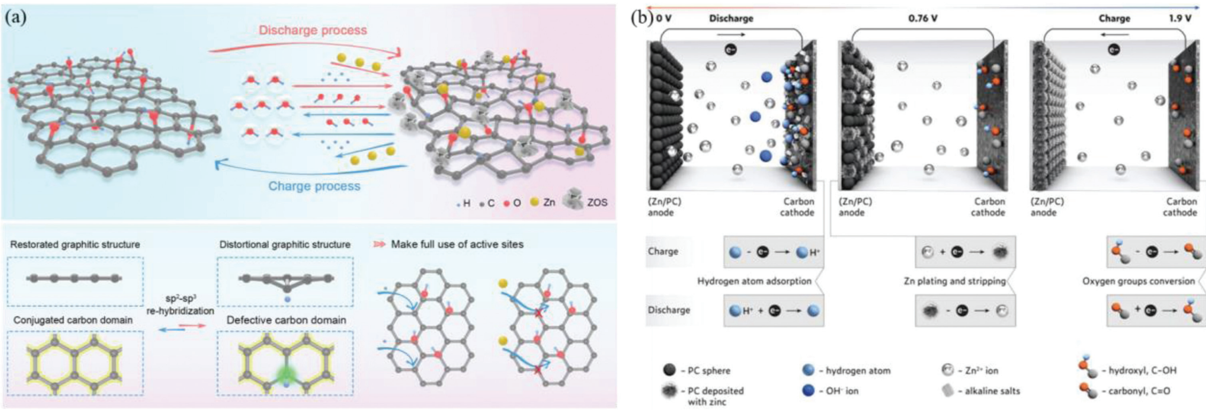

Fig. 2. (a) Schematic diagram for H^+ sorption on C atoms of the graphitic domains. Copied with permission [31]. Copyright 2022, Wiley-VCH GmbH. (b) Schematic illustration showing the Zn^{2+}/H^+ co-action storage mechanism. Copied with permission [17]. Copyright 2020, Wiley-VCH GmbH.

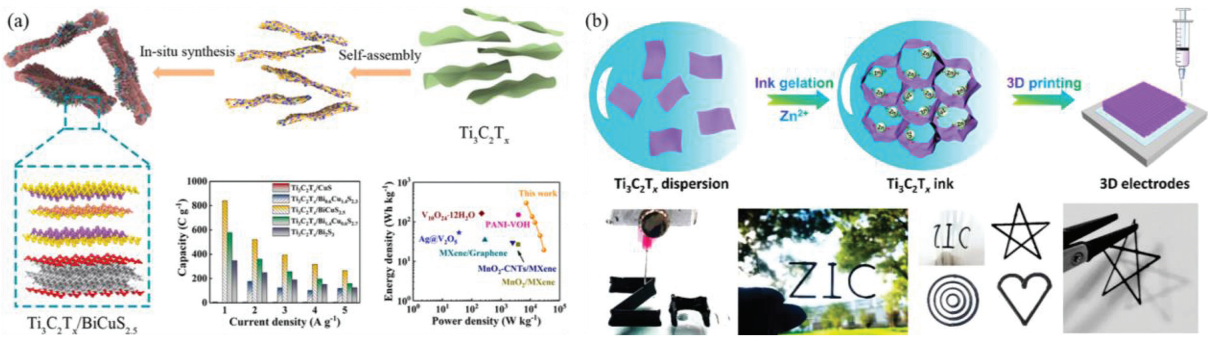

Fig. 3. (a) Synthetic illustration of the $BiCuS_{2.5}/Ti_3C_2T_x$ electrode material. Copied with permission [57]. Copyright 2021, Elsevier. (b) Synthetic illustration of a 3D-printed additive-free MXene cathode. Copied with permission [58]. Copyright 2021, American Chemical Society.

investigated pseudocapacitive electrode materials including transition metal oxides, carbides, nitrides, sulfides, *etc*. Very recently, a novel $BiCuS_{2.5}/Ti_3C_2T_x$ electrode material was designed based on a simple deposition route (Fig. 3a), and the as-assembled ZIC cell exhibited an improved energy density up to 298.4 Wh/kg@7.2 kW/kg [57]. Amorphous $BiCuS_{2.5}$ possessed the outstanding electrochemical reaction activity due to reversible redox reactions, and both the XPS analysis and theoretical simulation ascribed the working mechanism to the co-existence of intercalation pseudocapacitance and redox battery-like capacity. Moreover, MXenes as a prominent category of 2D transition metal (Ti, Nb, V, Cr, Mo, *etc.*) carbides/nitrides, are frequently applied in ZICs as the capacitor-type electrode materials [21,57–65]. 2D MXene structures can provide plentiful electroactive sites for redox pseudocapacitive reactions, in which ion penetration occurs between MXene sheets owing to the unbreakable chemical bonds, ultimately occupying active sites on the MXene surface for energy storage [60,61,66,67]. For example, a 3D-printed additive-free MXene cathode was developed through a facile gelation process for ZIC applications (Fig. 3b), and the resultant cathode delivered a dual-ion storage mechanism to combine the Zn^{2+} sorption process with H^+ pseudocapacitive behaviors ($Ti_3C_2O_2 + e^- + H^+ \leftrightarrow Ti_3C_2O(OH)$; $Ti_3C_2O_2 + 2e^- + 2H^+ \leftrightarrow Ti_3C_2(OH)_2$) [58]. The final MXene//Zn ZIC device exhibited a competitive energy-power output (0.10 mWh/cm^2@5.90 mW/cm^2) as well as a long cycling lifespan.

3. Battery-type electrodes in high-energy ZICs

Battery-type electrodes store energy by means of the intercalation/deintercalation reaction of cations into the internal electrode structure, and are divided into conventional metal Zn anodes and other battery-type materials like Mn/V-based oxides, Prussian blue analogues, organic compounds. The broadly-defined ZICs using conventional metal Zn anode or other battery-type electrode materials promise complementary high-energy output, while the diffusion-dominated working mechanism leads to unsatisfactory power density; meanwhile, the structure distortion induced by the phase evolution of the battery material also degrades the ion/electron dynamics (diffusion rate) [6,7,19]. Therefore, great research efforts have been devoted toward accelerating ion/electron dynamics in aqueous/non-aqueous electrolytes by surface modification or architecture exploration to fabricate high-rate battery-type electrodes without sacrificing high-energy density characteristic of zinc-ion batteries.

3.1. Metal Zn anode

Metal Zn is the most commonly-used anode material in conventional ZICs, where Zn^{2+} deposition/stripping on the battery-type Zn anode promises complementary high-energy density [9,10,17]. Upon charging, Zn^{2+} electrolyte-ions are deposited on the Zn anode, while Zn stripping occurs with Zn^{2+} diffusion to the electrolyte in the discharge process ($Zn \leftrightarrow Zn^{2+} + 2e^-$) [10,19]. Compared with the high-power capacitor-type electrode, the metal Zn anode still suffers from the low diffusion rate of Zn^{2+} caused by the structure distortion (Zn dendrite/corrosion/passivation) and poor Zn^{2+} deposition/stripping efficiency [22–24]. Consequently, versatile design strategies of metal Zn anode have been proposed in terms of electroplating architecture exploration, polymer/carbon surface coating and substrate/host composite [21–23,42,58,68–71]. For instance, Cha's group constructed a 2D nanostructured Zn anode based ZIC through a voltage-regulated electroplating technique (Fig. 4a) [22]. Such unique Zn architecture gave rise to reduced Zn^{2+}-diffusion routes and the enlarged surface area for the

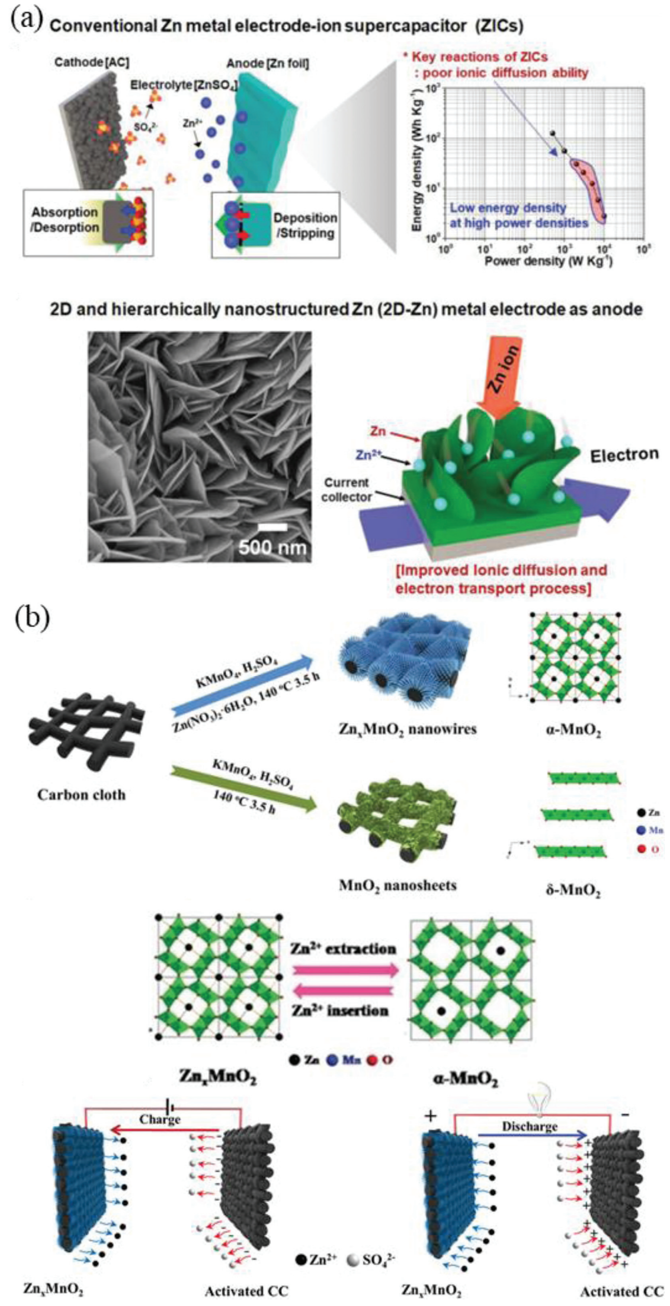

Fig. 4. (a) Schematic illustration of a 2D nanostructured Zn anode based ZIC. Copied with permission [22]. Copyright 2019, Wiley-VCH GmbH. (b) Schematic illustration of a Zn_xMnO_2 nanowires//AC ZIC. Reproduced with permission [75]. Copyright 2020, Wiley-VCH GmbH.

power density up to 20 kW/kg and a high energy density of 208 Wh/kg. So far, owing to the heterogeneous/dendritic Zn deposition, Zn dendrite growth on the pristine foil is the main challenge for metal Zn anode in current ZICs to raise safety concerns and impede Zn utilization efficiency [16,68,69,71]. Besides, the dendrite growth triggers disadvantageous Zn corrosion/passivation at the electrolyte-electrode interface, and further decreases the service lifespan of ZICs [71,72]. The Zn anode could be stabilized by a hydrophilic adhesive coating to block the formation of Zn dendrite on the modified Zn surface, and the resultant polymer coating layer presented uniform carbonyl Zn-deposition sites, thereby equipping the assembled ZICs with the capacity retention of 100% after 14000 cycles [68]. Moreover, a series of porous Zn@substrate/host composites using Ti_3C_2 film, Cu foil and MOF-derived materials, are involved as the conductive scaffolds to increase the Zn electrochemical utilization and afford homogeneously-distributed active sites for Zn nucleation [43,58,69,71,73,74]. Xia's group reported the dendrite-free Zn anode with a MOF ZIF-8 derived host [69]. After the calcination, Zn^{2+} within ZIF-8 was transformed into well-dispersed Zn throughout the inherent porous framework to serve as the deposition nuclei. By coupling the as-prepared anode material with an AC cathode, the ZIC cell exhibited excellent energy delivery (140.8 Wh/kg) while maintaining 72% capacity after 20000 turns, which would open up a highly-efficient route for *in-situ* fabrication of high-rate metal Zn anodes.

3.2. Other battery-type materials

Compared with conventional ZICs merely using metal Zn as the anode, current ZICs are broadly defined as the hybrid system consisting of a capacitor-type electrode and a battery-type electrode in a zinc-based electrolyte solution [9,13]. Beyond metal Zn, other battery-type electrode materials used in zinc-ion batteries are expected to proceed Zn^{2+} insertion/extraction in ZICs, such as Mn/V-based oxides, Prussian blue analogues (PBA), redox-active organic compounds [13,59,75–80]. Upon discharging, Zn^{2+} electrolyte-ions are inserted into the crystal structure of the battery-type electrode, while Zn^{2+} extraction occurs with subsequent diffusion to the electrolyte in the charge process [13,75]. Such broadly-defined ZICs can readily operate at higher voltages of 2 V for greater energy density than conventional ZICs, and the Zn(-dendrite)-free electrodes offer a high degree of freedom in material discovery and performance improvement. Mn/V-based oxides are the most commonly-used cathode materials in zinc-ion batteries due to various crystal structures and multivalent phases [6,16,81]. As the pioneer of the broadly-defined ZICs, Kang's group assembled the novel γ-MnO_2 nanorods//2 mol/L $ZnSO_4$//AC ZIC operated under 0-2 V, and the upgraded ZIC in the Mn^{2+}-containing $ZnSO_4$ electrolyte delivered the increased energy density from 34.8 Wh/kg to 83.8 Wh/kg [13]. Also, the SO_4^{2-} replacement with $CF_3SO_3^-$ in the electrolyte relieved side reactions including continuous Mn^{2+} dissolution and $Zn_4(OH)_6SO_4{\cdot}nH_2O$ byproduct formation on the MnO_2 electrode. So far, inferior electrical conductivity and structure/phase evolution are the main challenge for emerging battery-type materials in current ZICs to influence the Zn^{2+}/electron diffusion rate upon electrochemical turns [75,82]. Consequently, some regulation strategies have been developed, including fabricating stable crystal structures, and compositing with conductive materials (*e.g.*, CNTs, graphene, MXene) [59,63,75,83]. Recently, a Zn^{2+} pre-intercalation strategy was proposed to improve the tunnel structure stability of the battery-type MnO_2-based electrode for a high-performance ZIC with a remarkable battery-level energy density of 969.9 μWh/cm^2 and a power density up to 20.1 mW/cm^2 [75]. In this Zn_xMnO_2 nanowires//AC ZIC, Zn^{2+} insertion/extraction within Zn_xMnO_2 nanowire cathode (Zn_xMnO_2 – $2e^- \leftrightarrow Zn_yMnO_2 + Zn^{2+}$) worked with ion sorption on the AC anode to jointly achieve the excellent electrochemical performances (Fig. 4b). Ma's group reported a novel aqueous ZIC based on MXene anode and MnO_2@CNTs cathode, in which the energy and power densities reached 98.6 Wh/kg (77.5 W/kg) and 2480.6 W/kg (29.7 Wh/kg) [59]. Meanwhile, fabricating the MnO_2-based composite cathode with conductive CNTs could alleviate conductivity weaknesses and improve the framework strength for better cycle stability and Coulombic efficiency over 93.3% during 15000 cycles. Moreover, inspired by zinc-ion batteries, more innovative and comprehensive investigations into battery-type electrodes for ZICs are needed to diversify active electrode materials and energy storage mechanisms. For example, the intercalation-type PBA electrodes like $CoFe(CN)_6$ addressed the low-capacity drawback of

PBA-based zinc-ion batteries by multiple high-voltage redox-active centers for improved energy output [77]. The coordination-type redox-active organic compound electrodes (carbonyl/imine compounds, nitronyl nitroxides, triphenylamine derivatives, organosulfur/conductive polymers, *etc.*) could be equipped with plentiful coordination centers throughout the hierarchical configuration for Zn^{2+} interaction [79,84–89].

In-depth research efforts are still underway to explore dual-ion (co-)intercalation, redox-active coordination, and conversion mechanisms for advanced ZICs [16,90]. Multivalent Zn^{2+} charge carriers can deliver two-electron transfer during redox reaction for a high energy density of current ZICs, where Zn^{2+} insertion/extraction and Zn^{2+}/anion sorption occur at the battery-type and capacitor-type electrode interfaces, respectively. Also, the limited Zn^{2+} diffusion rate and strong electrostatic repulsion could degrade the charge storage and dynamics of current ZICs. Thus, the co-action storage mechanisms involving other charge carriers (H^+/anions/electrolyte-additive ions) with small ion sizes and rapid dynamics are highly-praised. The hydrogen redox reaction results in H^+ pseudocapacitive behaviors, while the consumption of H^+ charge carriers could be accompanied by the OH^--induced precipitation/dissolution of byproducts (alkaline zinc salts). The predominant involvement of anions in the Zn^{2+}-based solvated structure is expected to give the anionic co-insertion mechanism for high-performance reaction dynamics and structure reversibility.

4. Electrolytes in advanced ZICs

Capacitor-type and battery-type electrodes in ZICs have been discussed in the above two sections for high specific capacity and high diffusion rate, respectively. Further, in this section, new types of electrolytes including aqueous electrolytes, ionic liquid and organic electrolytes, and (*quasi*-)solid-state electrolytes, are presented to resolve the specific capacity and dynamics (diffusion rate) mismatch for advanced ZICs. The involved zinc salts in the electrolyte solutions are $ZnCl_2$, $Zn(CF_3SO_3)_2$, $ZnSO_4$, $Zn(NO_3)_2$, $ZnAc_2$, $Zn(ClO_4)_2$ and so on [19,20,24,91,92]. Among them, $ZnSO_4$ and $Zn(CF_3SO_3)_2$ are the most commonly used in current ZICs. Zhi's group investigated the influence of various anions carriers on the electrochemical behaviors of Zn//TiN ZICs, which demonstrated that SO_4^{2-} anions with the lowest negative adsorption energy were involved in the two-step adsorption-intercalation process to deliver the highest capacitance [24]. In contrast, the $Zn(CF_3SO_3)_2$ solution was proven to give the better anodic stability and high-efficiency Zn^{2+} deposition/stripping, owing to the fact that large $CF_3SO_3^-$ anions could block more surrounding H_2O molecules for the decreased solvation effect [19].

4.1. Aqueous electrolytes

Aqueous electrolyte ZICs prevail over ionic liquid and organic electrolyte counterparts relying on excellent ionic conductivity, high cost-effective and safe operational conditions [19,54,93]. Water-in-salt electrolytes have been frequently applied to upgrade the operational potential of aqueous zinc-based systems [18,54,94–97]. Super-concentrated salt solutions relieve the electrode-electrolyte interphase from H_2O availability, thereby broadening the electrochemical stability window over the thermodynamical range [54,94,98]. In a hybrid water-in-salt electrolyte (1 mol/kg $Zn(TFSI)_2 + 20$ mol/kg LiTFSI), where Zn^{2+} was blocked by $TFSI^-$ from H_2 evolution, dendrite-free Zn^{2+} deposition/stripping at nearly 100% Coulombic efficiency was demonstrated [18]. Ji's group developed a 30 mol/kg $ZnCl_2$ water-in-salt electrolyte to improve the Zn^{2+}-insertion potential and drag the anion-insertion potential lower, finally enlarging the operational potential window by 0.35 V in contrast to a 5 mol/kg dilute solution [95]. Recently, a phosphorene-based ZIC with 1 mol/kg $Zn(TFSI)_2 + 21$ mol/kg LiTFSI hybrid water-in-salt electrolyte delivered an operational voltage of up to 2.2 V and a capacitance of 214.3 F/g over 5000 charging-discharging cycles; the addition of a 0.2 mol/kg $ZnCl_2$-containing organic solvent further increased the voltage range to 2.5 V [54]. Another solution to upgrade the operational potential of aqueous ZICs is to introduce soluble electrolyte additives into dilute solutions [13,93,99]. The addition of metal salts can shield a small amount of Zn^{2+} in zinc-based aqueous electrolytes, or control the dendrite growth by co-deposition with Zn. Fan's group supplemented Mg^{2+} cations into a common 2 mol/L $ZnSO_4$ aqueous electrolyte for the invertible $Zn_4SO_4(OH)_6{\cdot}xH_2O$ formation in ZICs. For the Zn anode, the Mg^{2+} cation-mediated electrolyte was proven to suppress the hydrogen evolution for homogeneous Zn nucleation-deposition under high voltage, while ion sorption and invertible proton adsorption related to the $Zn_4SO_4(OH)_6{\cdot}xH_2O$ formation led to high capacity for the AC cathode [93]. Besides, the addition of redox couples to electrolytes can further supplement extra charge carriers to take advantage of the "dead" mass of electrolytes for faradaic reactions, and organic anions like OTF^-, $TFSI^-$ are compelled in the Zn^{2+} solvation structure to kinetically prevent H_2O-related side reactions [18,99–102].

4.2. Ionic liquid and organic electrolytes

Ionic liquid and organic electrolytes are also frequently mentioned in ZICs because of the high-potential and wide-temperature durability [36,103,104]. In such electrolytes, the involved organic solvents are acetonitrile, dimethyl sulfoxide, *N*,*N*-dimethylformamide and so on, and well-soluble $Zn(CF_3SO_3)_2$ is nowadays frequently selected as the electrolyte salt [36,105–107]. Deep eutectic solvents (DESs), as one type of ionic liquids, can be formed by a Lewis base (*e.g.*, urea, ethylene glycol, acetamide, succinonitrile) with a Lewis acid (LiTFSI, $Zn(TFSI)_2$, *etc.*) [103,108–111]. A high flexibility in constituent type and molar percentage endows DESs with lower melting/phase-transition points, and the unique H-bonding network in DESs can confine most of H_2O molecules to the matrix for expanded operational potential [108,112]. For instance, a water-in-DES (urea/LiTFSI/$Zn(TFSI)_2$) electrolyte was developed, wherein the suppressed water reactivity enabled durable Zn^{2+} deposition/stripping with greatly improved cycling stability in contrast with routine electrolytes (Fig. 5a) [108]. Fan's group reported a novel hydrated DES electrolyte consisting of $Zn(ClO_4)_2$, methylsulfonylmethane and H_2O, where the Lewis base (methylsulfonylmethane) coordinated the Zn^{2+} solvation shell with H_2O molecules [103]. The solvated structure and eutectic interaction in such an electrolyte system resulted in the dendrite-free Zn deposition, which could give inspiring insights into the structure-performance relation between the solvation effect in DES electrolytes and electrochemical parameters like cycle reversibility, potential/temperature durability.

4.3. (Quasi-)solid-state electrolytes

(*Quasi*-)solid-state electrolytes with fascinating mechanical stability and temperature durability, have aroused great interest in current ZICs to fit the ever-growing demand of versatile flexible and portable electronics [20,21,34,78,92,113–118]. A $ZnCl_2$ polyacrylamide hydrogel electrolyte was proposed, and the Cl^- desolvation energy induced the smaller $[ZnCl]^+(H_2O)_{n-1}$ (with $n = 1$-6) clusters for higher cathode capacity (Fig. 5b) [20]. The resultant ZIC using the hydrogel electrolyte delivered the energy density of 217 Wh/kg@450 W/kg, coupled with low-temperature adaptability and mechanical flexibility (92.9% capacitance retention upon 40000 cycles at −20 °C). A robust *quasi*-solid-state ZIC was assembled by fabricating a $Zn(ClO_4)_2$ poly(vinyl alcohol) (PVA) hy-

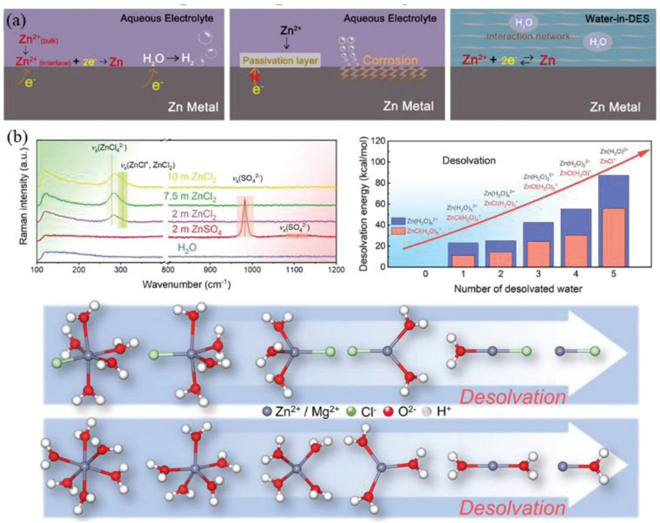

Fig. 5. (a) Schematic diagrams of metal Zn anode in the aqueous and water-in-DES electrolytes. Copied with permission [108]. Copyright 2019, Elsevier. (b) Raman spectra of $ZnCl_2$ electrolytes with different concentrations, desolvation energies of $[Zn(H_2O)_6]^{2+}/[ZnCl(H_2O)_5]^{+}$, the illustration of the $Zn^{2+}/ZnCl^{+}$ desolvation. Copied with permission [20]. Copyright 2020, Wiley-VCH GmbH.

drogel electrolyte, where $Zn(ClO_4)_2$ attracted a large number of free H_2O molecules through H-bonding interactions [92]. Consequently, the flexible device retained the superior storage capacity and cycling reversibility at a low operational temperature of −50 °C, revealing exceptional anti-freezing performance. Electrolyte additives like organic molecules and polymers in (*quasi*-)solid-state electrolytes can suppress Zn dendrite and other side effects by engineering current distribution and ion transfer. Ethylene glycol is applied as a common additive antifreeze and holds great promise to inhibit dendrite formation, due to the low water content and uniform Zn-deposition sites mediated by organic material additions. A series of $ZnSO_4$-based hybrid electrolytes with ethylene glycol as the antifreeze agent was reported, wherein the solvation interaction between ethylene glycol and Zn^{2+} gave the hybrid electrolytes with a decreased freezing point and high-efficiency Zn^{2+}/Zn chemistry (Fig. 6a) [117]. Yang's group designed a self-catalytic nano-reinforced system to synthesize a $ZnCl_2$ polyzwitterionic hydrogel electrolyte for low-temperature flexible ZICs (Fig. 6b) [118]. The polyzwitterionic network filled with $ZnCl_2$ reduced the ion-transfer barriers for the high-rate Zn anode to relieve side reactions and extend service durability, which offered innovative fabricating ideas for high-performance ZICs in applications of flexible and portable electronics across a wide adaptive temperature range.

5. Conclusions and outlook

Zinc-ion energy storage systems hold great promise for the merits of abundant natural reserves, high theoretical gravimetric capacity, low electrochemical potential, operational safety, *etc.* ZICs are considered as one competitive candidate with the congenerous features of both supercapacitors and zinc-ion batteries, targeting a combination of high-power delivery, high-energy output and high-quality service durability. In this mini-review, recent advances in both electrodes and electrolytes of ZICs are versatilely concluded to remedy the specific capacity and dynamics (diffusion rate) mismatch owing to the hybrid energy storage mechanism. Based on the surface-dominated working mechanism, capacitor-type electrodes are upgraded by porous/dimensional structure engineering (surface accessibility) or doping redox-active constituents (surface pseudocapacitance) to bridge the capacity gap. Meanwhile, battery-type electrodes relying on the diffusion-dominated working mechanism are tailor-designed by surface modification or architecture exploration to relieve the structure/phase evolution especially upon high-rate/successive electrochemical turns. Furthermore, electrolyte research referring to aqueous electrolytes, ionic liquid and organic electrolytes and (*quasi*-)solid-state electrolytes is presented to broaden ZIC exploitation toward advanced performances like high operational potential and wide adaptive temperature. Despite great achievements in the past few years, the practical application of rising ZICs still cannot meet the ever-growing indicator demand. More forceful and comprehensive efforts are in dire need, and the next-stage research directions are outlined as follows.

(1) For the role of high-capacity capacitor-type electrodes, more attention should be paid to increasing the electrochemical active surface area (surface accessibility and surface pseudocapacitance) rather than the specific surface area. In terms of surface accessibility, only shallow sorption sites on the electrode skeleton are readily accessed by electrolyte species to give immediate capacitive responses; consequently, *in situ* optimization strategies of preset precursor skeletons are highly praised to build 3D hierarchical porous carbon architectures, where interconnected meso-/macropores can reduce migration barriers into deep sorption sites on interior surface. In terms of surface pseudocapacitance, the working mechanisms related to heteroatom dopant sites re-

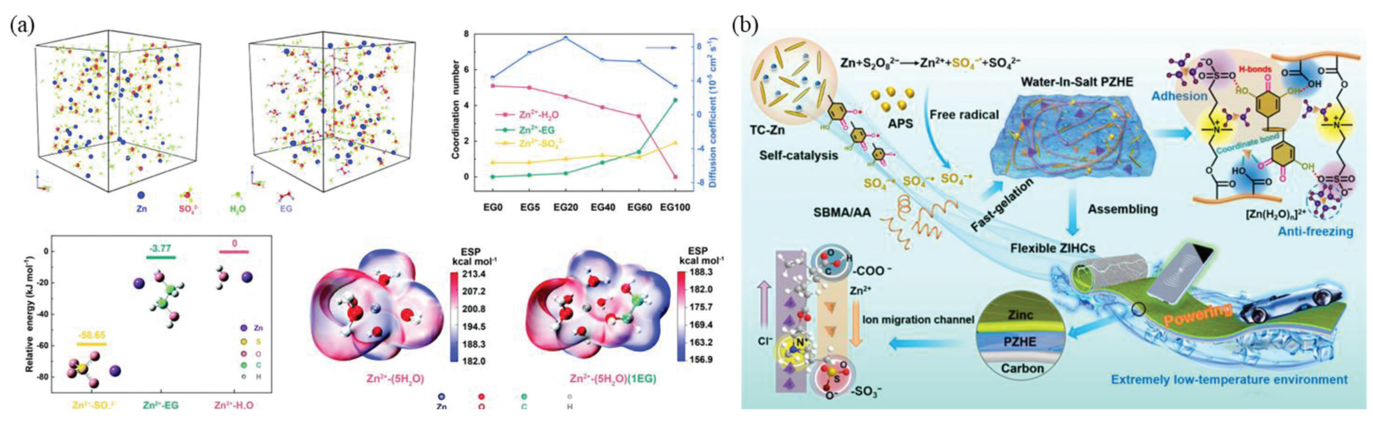

Fig. 6. (a) Optimized structure of $ZnSO_4$-based hybrid electrolytes with ethylene glycol. Copied with permission [117]. Copyright 2020, the Royal Society of Chemistry. (b) Synthetic illustration of a $ZnCl_2$ polyzwitterionic hydrogel electrolyte for low-temperature flexible ZICs. Copied with permission [118]. Copyright 2021, American Chemical Society.

quire further clarification, since current ZICs have only reported redox pseudocapacitive reactions between Zn^{2+} and O-containing functionalities; more simulation characterizations and theoretical calculations shall help to understand the interfacial sorption dynamics and the interaction of versatile dopants. Besides, novel and high-quality pseudocapacitive materials should be explored including transition metal compounds and other potential pseudocapacitive layered architectures.

(2) With regard to high-rate battery-type electrodes, the structure/phase evolution originated from the battery-type working mechanism is the main concern ion/electron diffusion rate degradation. Metal Zn anodes are mostly plagued by Zn dendrite growth and poor Zn^{2+} deposition/stripping efficiency, while other batter-type electrodes are also challenged by continuous cathode dissolution and byproduct (*e.g.*, $Zn_4(OH)_6SO_4{\cdot}nH_2O$) formation. Consequently, the next-stage research can be centered on architecture exploration, surface coating and substrate/host composite for better cycling/power properties; further, the above-mentioned robust capacitor-type material structures can also serve as the conductive scaffolds to participate in the tailor-design of emerging battery-type electrodes to remedy the inferior electrical conductivity and unreversible structure/phase evolution. Moreover, inspired by zinc-ion batteries, more innovative and comprehensive investigations into battery-type electrodes for ZICs are needed to diversify active electrode materials (intercalation-type PBAs, coordination-type redox-active organic compounds, *etc.*) and energy storage mechanisms such as (co-)intercalation/coordination/conversion mechanisms.

(3) Considering advanced aqueous/non-aqueous electrolytes, high-quality service durability can be realized by electrolyte exploitation to boost the operational potential and widen the adaptive temperature. $ZnSO_4$ and $Zn(CF_3SO_3)_2$ are the most commonly used zinc electrolyte salts in current ZICs. Water-in-salt electrolytes not only inherit the environmental friendliness and safe/facile operational condition characteristic of conventional aqueous electrolytes, but also upgrade the operational potential by relieving the electrode-electrolyte interphase from H_2O availability. The supplement of soluble electrolyte additives into dilute solutions can better utilize the "dead" mass of electrolytes and kinetically prevent H_2O-related side reactions. And novel electrolyte salts like $ZnCl_2$, $ZnAc_2$, and $Zn(ClO_4)_2$ are promising to overcome the precipitation/dissolution of zinc salt byproducts (*e.g.*, $Zn_4(OH)_6SO_4{\cdot}nH_2O$). Moreover, ionic liquid and organic electrolytes further promote ZIC advances with higher-potential and wider-temperature durability. The synthesis flexibility and unique H-bonding network of DESs result in lower melting/phase-transition points and powerful H_2O constraints in ultimate ZICs. Besides, (*quasi*-)solid-state electrolytes with fascinating mechanical stability and temperature durability, appear to resolve Zn dendrite growth and unreversible electrode dissolution.

(4) To keep pace with the fast-changing development of the portable electronics era, fabricating flexible ZICs integrated with new features and smart functions represents a vital research direction for practical applications, such as photo-chargeable, shape-memory, stretchable and biodegradable ZIC devices. The current zinc-ion technology holds a potential position in the market dominance of power-backup applications like Internet hubs or cellular repeater towers, wherein multi-functional flexible ZICs are the emerging candidates to power portable smart equipment. The equipment processability/scalability is highly required for fundamental researches and practical applications, so advanced fabrication routes including 3D printing, inkjet/screen printing and laser etching, are preferred for the development of next-generation ZICs.

Declaration of competing interest

The authors declare that they have no known competing financial interests or personal relationships that could have appeared to influence the work reported in this paper.

Acknowledgments

This work was financially supported by the National Natural Science Foundation of China (Nos. 21875165, 21905207, 22172111, and 51772216), the Science and Technology Commission of Shanghai Municipality, China (Nos. 22ZR1464100, 20ZR1460300, and 19DZ2271500), Zhejiang Provincial Natural Science Foundation of China (No. LY19B010003), and the Fundamental Research Funds for the Central Universities.

References

[1] P. Simon, Y. Gogotsi, Nat. Mater. 19 (2020) 1151–1163.
[2] J. Xiao, J.W. Han, C. Zhang, et al., Adv. Energy Mater. 12 (2022) 2100775.
[3] Y.Y. Liu, X. Lu, F.L. Lai, et al., Joule 5 (2021) 2845–2903.
[4] H. Shao, Y.C. Wu, Z. Lin, et al., Chem. Soc. Rev. 49 (2020) 3005–3039.
[5] J.Z. Wu, Chem. Rev. 122 (2022) 10821–10859.
[6] D. Tie, S. Huang, J. Wang, et al., Energy Storage Mater. 21 (2019) 22–40.
[7] N.R. Chodankar, H.D. Pham, A.K. Nanjundan, et al., Small 16 (2020) 2002806.
[8] P. Geng, L. Wang, M. Du, et al., Adv. Mater. 34 (2022) 2107836.
[9] H. Wang, W. Ye, Y. Yang, et al., Nano Energy 85 (2021) 105942.
[10] Y. Tian, R. Amal, D.W. Wang, Front. Energy Res. 4 (2016) 34.
[11] Y. He, P. Zhang, M. Wang, et al., Mater. Horiz. 6 (2019) 1041–1049.
[12] L. Dong, X. Ma, Y. Li, et al., Energy Storage Mater. 13 (2018) 96–102.
[13] X. Ma, J. Cheng, L. Dong, et al., Energy Storage Mater. 20 (2019) 335–342.
[14] Q.Y. Dou, N.Z. Wu, H. Yuan, et al., Chem. Soc. Rev. 50 (2021) 6734–6789.
[15] Z. Song, G. Zhang, X. Deng, et al., Nano-Micro Lett. 14 (2022) 53.
[16] H. Li, L. Ma, C. Han, et al., Nano Energy 62 (2019) 550–587.
[17] J. Yin, W. Zhang, W. Wang, et al., Adv. Energy Mater. 10 (2020) 2001705.
[18] F. Wang, O. Borodin, T. Gao, et al., Nat. Mater. 17 (2018) 543–549.
[19] S. Wu, Y. Chen, T. Jiao, et al., Adv. Energy Mater. 9 (2019) 1902915.
[20] C. Wang, Z. Pei, Q. Meng, et al., Angew. Chem. Int. Ed. 60 (2021) 990–997.
[21] Q. Yang, Z. Huang, X. Li, et al., ACS Nano 13 (2019) 8275–8283.
[22] G.H. An, J. Hong, S. Pak, et al., Adv. Energy Mater. 10 (2019) 1902981.
[23] P. Zhang, Y. Li, G. Wang, et al., Adv. Mater. 31 (2019) 1806005.
[24] Z. Huang, T. Wang, H. Song, et al., Angew. Chem. Int. Ed. 60 (2021) 1011–1021.
[25] Y. Qin, L. Miao, M. Mansuer, et al., ACS Appl. Mater. Interfaces 14 (2022) 33328–33339.
[26] Z. Song, L. Miao, L. Li, et al., Carbon 180 (2021) 135–145.
[27] Z. Song, L. Miao, L. Ruhlmann, et al., Adv. Mater. 33 (2021) 2104148.
[28] H. He, J. Lian, C. Chen, et al., Nano-Micro Lett. 14 (2022) 106.
[29] H. Li, J. Wu, L. Wang, et al., Chem. Eng. J. 428 (2022) 131071.
[30] R. Fei, H. Wang, Q. Wang, et al., Adv. Energy Mater. 10 (2020) 2002741.
[31] H. Xu, W. He, Z. Li, et al., Adv. Funct. Mater. 32 (2022) 2111131.
[32] M. Mansuer, L. Miao, Y. Qin, et al., Chin. Chem. Lett. 34 (2023) 107304.
[33] Y. Wang, Y. Zeng, J. Zhu, et al., Colloid Surf. A 649 (2022) 129356.
[34] C.C. Hou, Y. Wang, L. Zou, et al., Adv. Mater. 33 (2021) 2101698.
[35] J. Zeng, L. Dong, L. Sun, et al., Nano-Micro Lett. 13 (2020) 19.
[36] X. Qiu, N. Wang, Z. Wang, et al., Angew. Chem. Int. Ed. 60 (2021) 9610–9617.
[37] X. Zheng, L. Miao, Z. Song, et al., J. Mater. Chem. A 10 (2022) 611–621.
[38] H. Zhang, Q. Liu, Y. Fang, et al., Adv. Mater. 31 (2019) 1904948.
[39] X. Deng, J. Li, Z. Shan, et al., J. Mater. Chem. A 8 (2020) 11617–11625.
[40] G. Ping, L. Miao, A. Awati, et al., Chin. Chem. Lett. 32 (2021) 3811–3816.
[41] L. Zhang, D. Wu, G. Wang, et al., Chin. Chem. Lett. 32 (2021) 926–931.
[42] G. Sun, H. Yang, G. Zhang, et al., Energ. Environ. Sci. 11 (2018) 3367–3374.
[43] X. Zhang, Z. Pei, C. Wang, et al., Small 15 (2019) 1903817.
[44] Q. Guo, Y. Han, N. Chen, et al., ACS Energy Lett. 6 (2021) 1786–1794.
[45] L. Miao, H. Duan, D. Zhu, et al., J. Mater. Chem. A 9 (2021) 2714–2724.
[46] Z. Song, G. Zhang, X. Deng, et al., Adv. Funct. Mater. 32 (2022) 2205453.
[47] X. Deng, K. Zou, R. Momen, et al., Sci. Bull. 66 (2021) 1858–1868.
[48] Y. Shao, Z. Sun, Z. Tian, et al., Adv. Funct. Mater. 31 (2021) 2007843.
[49] Y. Li, P. Lu, P. Shang, et al., J. Energy Chem. 56 (2021) 404–411.
[50] H. Duan, Z. Song, L. Miao, et al., J. Mater. Chem. A 10 (2022) 9837–9847.
[51] X. Zhang, Y. Zhang, J. Qian, et al., Nanoscale 14 (2022) 2004–2012.
[52] Y. Lu, Z. Li, Z. Bai, et al., Nano Energy 66 (2019) 104132.
[53] B.D. Boruah, A. Mathieson, B. Wen, et al., Nano Lett. 20 (2020) 5967–5974.
[54] Z. Huang, A. Chen, F. Mo, et al., Adv. Energy Mater. 10 (2020) 2001024.
[55] L. Dong, W. Yang, W. Yang, et al., Nano-Micro Lett. 11 (2019) 94.

[56] S.J. Patil, N.R. Chodankar, S.K. Hwang, et al., Energy Storage Mater. 45 (2022) 1040–1051.
[57] Y. Li, W. Zhang, X. Yang, et al., Nano Energy 87 (2021) 106136.
[58] Z. Fan, J. Jin, C. Li, et al., ACS Nano 15 (2021) 3098–3107.
[59] S. Wang, Q. Wang, W. Zeng, et al., Nano-Micro Lett. 11 (2019) 70.
[60] X. Li, M. Li, Q. Yang, et al., Adv. Energy Mater. 10 (2020) 2001394.
[61] L. Ding, Y. Wei, L. Li, et al., Nat. Commun. 9 (2018) 155.
[62] F. Li, Y. Liu, G. Wang, et al., Chem. Eng. J. 435 (2022) 135052.
[63] J. Shi, S. Wang, Q. Wang, et al., J. Power Sources 446 (2020) 227345.
[64] C. Wang, S. Wei, S. Chen, et al., Small Methods 3 (2019) 1900495.
[65] A.S. Etman, J. Halim, J. Rosen, Mater. Today Energy 22 (2021) 100878.
[66] C. Liu, Y. Bai, W. Li, et al., Angew. Chem. Int. Ed. 61 (2022) e202116282.
[67] Y. Bai, C. Liu, T. Chen, et al., Angew. Chem. Int. Ed. 60 (2021) 25318–25322.
[68] B. Niu, Z. Li, S. Cai, et al., Chem. Eng. J. 442 (2022) 136217.
[69] Z. Wang, J. Huang, Z. Guo, et al., Joule 3 (2019) 1289–1300.
[70] P. Liu, X. Fan, B. Ouyang, et al., J. Power Sources 518 (2022) 230740.
[71] M. Kwon, J. Lee, S. Ko, et al., Energy Environ. Sci. 15 (2022) 2889–2899.
[72] J. Jin, X. Geng, Q. Chen, et al., Nano-Micro Lett. 14 (2022) 64.
[73] C. Leng, Z. Zhao, J. Guo, et al., Chem. Commun. 57 (2021) 8778–8781.
[74] L. Dong, W. Yang, W. Yang, et al., Chem. Eng. J. 384 (2020) 123355.
[75] Q. Chen, J. Jin, Z. Kou, et al., Small 16 (2020) 2000091.
[76] B.D. Boruah, B. Wen, S. Nagane, et al., ACS Energy Lett. 5 (2020) 3132–3139.
[77] L. Ma, S. Chen, C. Long, et al., Adv. Energy Mater. 9 (2019) 1902446.
[78] Y. Jiang, K. Ma, M. Sun, et al., Energy Environ. Mater. 0 (2022) 1–8.
[79] Z. Xu, M. Li, W. Sun, et al., Adv. Mater. 34 (2022) 2200077.
[80] W. Yang, W. Yang, Y. Huang, et al., Chin. Chem. Lett. 33 (2022) 4628–4634.
[81] Y. Heng, Z. Gu, J. Guo, X. Wu, Acta Phys. Chim. Sin. 37 (2021) 2005013.
[82] J. Yin, W. Zhang, N.A. Alhebshi, et al., Adv. Energy Mater. 11 (2021) 2100201.
[83] W. Du, L. Miao, Z. Song, et al., J. Power Sources 536 (2022) 231512.
[84] Y. Zhao, Y. Huang, F. Wu, et al., Adv. Mater. 33 (2021) 2106469.
[85] Q. Zhao, W. Huang, Z. Luo, et al., Sci. Adv. 4 (2018) eaao1761.
[86] M. Yu, N. Chandrasekhar, R.K.M. Raghupathy, et al., J. Am. Chem. Soc. 142 (2020) 19570–19578.
[87] Y. Zhao, Y. Wang, Z. Zhao, et al., Energy Storage Mater. 28 (2020) 64–72.
[88] Z. Tie, Z. Niu, Angew. Chem. Int. Ed. 59 (2020) 21293–21303.
[89] Z. Song, L. Miao, H. Duan, et al., Angew. Chem. Int. Ed. 61 (2022) e202208821.
[90] P. Ruan, S. Liang, B. Lu, et al., Angew. Chem. Int. Ed. 61 (2022) e202200598.
[91] J. Eskusson, T. Thomberg, E. Lust, et al., J. Electrochem. Soc. 169 (2022) 020512.
[92] G. Yang, J. Huang, X. Wan, et al., Nano Energy 90 (2021) 106500.
[93] P. Wang, X. Xie, Z. Xing, et al., Adv. Energy Mater. 11 (2021) 2101158.
[94] L. Suo, O. Borodin, T. Gao, et al., Science 350 (2015) 938–943.
[95] X. Wu, Y. Xu, C. Zhang, et al., J. Am. Chem. Soc. 141 (2019) 6338–6344.
[96] J. Yan, L. Miao, H. Duan, et al., Chin. Chem. Lett. 33 (2022) 2681–2686.
[97] X. Qian, L. Miao, J. Jiang, et al., Chem. Eng. J. 388 (2020) 124208.
[98] C. Long, L. Miao, D. Zhu, et al., ACS Appl. Energy Mater. 4 (2021) 5727–5737.
[99] L. Han, H. Huang, J. Li, et al., J. Mater. Chem. A 8 (2020) 15042–15050.
[100] H. Luo, Y. Wang, G. Wang, et al., J. Power Sources 436 (2019) 226843.
[101] M. Mansuer, L. Miao, D. Zhu, et al., Mater. Chem. Front. 5 (2021) 3061–3072.
[102] L. Han, H. Huang, J. Li, et al., J. Mater. Chem. A 7 (2019) 24400–24407.
[103] M. Han, J. Huang, X. Xie, et al., Adv. Funct. Mater. 32 (2022) 2110957.
[104] Y. Wang, L. Hao, Y. Zeng, et al., J. Alloy. Compd. 886 (2021) 161176.
[105] H. Zhou, C. Liu, J.C. Wu, et al., J. Mater. Chem. A 7 (2019) 9708–9715.
[106] L. Zhang, Z. Liu, G. Wang, et al., Nanoscale 13 (2021) 17068–17076.
[107] M. Huang, A. Tang, Z. Wang, et al., Chin. Chem. Lett. 32 (2021) 2009–2012.
[108] J. Zhao, J. Zhang, W. Yang, et al., Nano Energy 57 (2019) 625–634.
[109] X. Bu, Y. Zhang, Y. Sun, et al., J. Energy Chem. 49 (2020) 198–204.
[110] F. Li, L. Yu, Q. Hu, et al., Sci. China Mater. 64 (2021) 1609–1620.
[111] L.I.N. Tomé, V. Baião, W. da Silva, et al., Appl. Mater. Today 10 (2018) 30–50.
[112] B. Wu, Y. Mu, Z. Li, et al., Chin. Chem. Lett. 34 (2023) 107629.
[113] Y. Sun, H. Ma, X. Zhang, et al., Adv. Funct. Mater. 31 (2021) 2101277.
[114] Q. Zhang, Y. Ma, Y. Lu, et al., Nat. Commun. 11 (2020) 4463.
[115] Z. Xu, R. Ma, X. Wang, Energy Storage Mater. 46 (2022) 233–242.
[116] H. Wang, X. Li, D. Jiang, et al., J. Power Sources 528 (2022) 231210.
[117] N. Chang, T. Li, R. Li, et al., Energy Environ. Sci. 13 (2020) 3527–3535.
[118] Q. Fu, S. Hao, L. Meng, et al., ACS Nano 15 (2021) 18469–18482.